

---


Retrospective Theses and Dissertations

---

1988

## Design of a bandpass oculometer

Karin Brandauer  
*University of Central Florida*

 Part of the [Systems and Communications Commons](#)  
Find similar works at: <https://stars.library.ucf.edu/rtd>  
University of Central Florida Libraries <http://library.ucf.edu>

This Masters Thesis (Open Access) is brought to you for free and open access by STARS. It has been accepted for inclusion in Retrospective Theses and Dissertations by an authorized administrator of STARS. For more information, please contact [STARS@ucf.edu](mailto:STARS@ucf.edu).

---

### STARS Citation

Brandauer, Karin, "Design of a bandpass oculometer" (1988). *Retrospective Theses and Dissertations*. 4263.  
<https://stars.library.ucf.edu/rtd/4263>

DESIGN OF A BANDPASS OCULOMETER

BY

KARIN BRANDAUER

B.S.E., University of Central Florida, 1986

THESIS

Submitted in partial fulfillment of the requirements  
for the degree of Master of Science in Engineering  
in the Graduate Studies Program  
of the College of Engineering  
University of Central Florida  
Orlando, Florida

Fall Term  
1988

## ABSTRACT

A passive oculometer is a device that measures the position of the eye by utilizing the corneo-retinal potential (CRP) generated by the eye. In this thesis, the Bandpass Oculometer replaces the joystick of a personal computer, allowing the viewer to use a computer simply by moving his eyes.

Low frequency noise, present in all electronic circuits, produces an offset from the reference point, the center of the screen. In previous lowpass oculometry studies at University of Central Florida, this offset caused the cursor to drift toward the edge of the field of view within a period of 30 seconds, decreasing the ability to precisely control the cursor on the monitor. The Bandpass Oculometer is different from its predecessors in that bandpass filtering is utilized. By filtering all frequencies except where eye movement occurs, low frequency drift noise and higher frequency interference signals are eliminated. Consequently, the viewer can achieve a reference with no offset and no drift, resulting in smoother tracking and better control of the computer.

An additional improvement to previous oculometers is

the new computer interface. A diode shaping network is used to simulate a joystick resistance, and an optocoupler relays the output current to the computer. The optocoupler electrically isolates the viewer from the computer, thus making the system safer to use.

## ACKNOWLEDGEMENTS

I would like to thank my parents and my friends who have been so supportive. Special thanks to Jack for all his love and understanding.

For my professional and educational achievements, I would like to thank Dr. Robert Martin, Dr. Michael Harris, Dr. Robert Walker, Dr. Richard Miller, and the University of Central Florida Electrical Engineering Department.

## TABLE OF CONTENTS

LIST OF FIGURES. . . . .	vi
LIST OF TABLES . . . . .	viii
INTRODUCTION . . . . .	1
Static Corneo-Retinal Potential . . . . .	1
Method of Collecting Charge . . . . .	3
Brief Summary of UCF Oculometry Studies . . . . .	4
Outline of Bandpass Oculometer. . . . .	5
SPECIFICATIONS . . . . .	7
Average Field of View . . . . .	7
Amplification Necessary . . . . .	7
Noise Considerations. . . . .	8
Bandwidth Selection . . . . .	10
Using Gameport to Access Computer . . . . .	11
Explanation of Gameport Circuitry . . . . .	11
Diode Shaping Network: Break Off Voltage and Slope Specifications . . . . .	14
SYSTEM DESIGN. . . . .	15
Instrumentation Amplifier . . . . .	15
Bandpass Filter . . . . .	16
Supplemental Gain . . . . .	20
Computer Interface. . . . .	21
RESULTS. . . . .	28
Instrumentation Amplifier . . . . .	28
Bandpass Filter . . . . .	29
Supplemental Gain . . . . .	33
Computer Interface. . . . .	33
System Test . . . . .	34
CONCLUSIONS AND RECOMMENDATIONS. . . . .	37
APPENDIX A . . . . .	39
APPENDIX B . . . . .	42
APPENDIX C . . . . .	46
APPENDIX D . . . . .	54
LIST OF REFERENCES . . . . .	59

## LIST OF FIGURES

1.	Static Corneo-Retinal Potential. . . . .	2
2.	Placement of Electrodes (a) on the face and (b) on the ski mask. . . . .	4
3.	Basic Block Diagram of Bandpass Oculometer . . . .	5
4.	Average Extreme Look Angles. . . . .	8
5.	Low Frequency Spectrum . . . . .	9
6.	Stopband Configuration of Bandpass Filter. . . .	10
7.	Paddle Position vs. Joystick Resistance. . . . .	13
8.	Classic Three Instrumentation Amplifier. . . . .	16
9.	Sallen and Key Lowpass Circuit (Second Order). .	19
10.	Bandpass Filter. . . . .	20
11.	Supplemental Gain. . . . .	21
12.	Diode Shaping Network. . . . .	23
13.	Simpler Version of Diode Shaping Network . . . .	24
14.	Break Off Voltage Circuitry. . . . .	24
15.	Optocoupler Network. . . . .	26
16.	Microcap AC Analysis . . . . .	30
17.	Frequency Response of Channel 1 (0-1 Hz) . . . .	31
18.	Frequency Response of Channel 1 (0-25 Hz). . . .	31
19.	Frequency Response of Channel 2 (0-1 Hz) . . . .	32
20.	Frequency Response of Channel 2 (0-25 Hz). . . .	32
21.	Transfer Response of the Diode Shaping Network .	34
22.	Measurement of Common Mode Gain. . . . .	41

23.	Measurement of Differential Mode Gain. . . . .	41
24.	Classic Three Instrumentation Amplifier. . . . .	43
25.	Sallen and Key Lowpass Stage (Second Order). . .	48
26.	Pole Locations of Unit Circle. . . . .	50
27.	Sallen and Key Highpass Stage (Second Order) . .	52
28.	Pole Reciprocation (a) Lowpass to (b) Highpass .	52



## LIST OF TABLES

1. Summary of Specifications . . . . .	14
2. Resistor Values for Instrumentation Amplifier . .	17
3. Component Values for Bandpass Filter. . . . .	19
4. Resistor Values for Supplemental Gain . . . . .	21
5. Parameters That Control Slope of Shaping Network.	25
6. Resistor Values for Computer Interface. . . . .	26
7. Common Mode Rejection Ratio for Instrumentation Amplifier. . . . .	28
8. Measurements for Supplemental Gain. . . . .	33

## INTRODUCTION

The oculometer is a device that measures the movement of an eye. Oculometers have many uses. For the military, an oculometer could help reduce pilot workload in the form of automatic target tracking, where the pilot only has to follow his target with his eyes; the oculometer then feeds the eye position information into a computer which, for example, may be connected to an automatic firing system. For the public, an oculometer could help a quadriplegic or other handicapped person use a computer. Most oculometers in use today are active, usually involving a beam of light to be shined into the eye. These active oculometers are very accurate due to the direct contact with the eye. However, these devices are expensive and may be distracting to the line of vision.

A less expensive method is a passive oculometer; by utilizing the static corneo-retinal potential (CRP) present in the eye, one can measure the position of the eyeball in reference to the head (Panayiotou 1984). The CRP is generated due to chemical activity between the retina and the cornea. Negative ions are present in the retina, while positive ions are distributed on the cornea as shown in

Figure 1. This charge distribution can be modeled as an electric dipole which generates a field according to Coulomb's law. As the eye, or dipole, is rotated, the field is changed. Usually, this field is dissipated through the skin; however, if electrodes are placed around the eye, these minute voltages (approximately 10 uv/degree eye movement) can be measured. In fact, the voltage measured by the electrodes is dependent upon the orientation of the eye in reference to the head. For example, if the eye is looking up, the field will be more dense above the eye than below, and more charge will be deposited on the electrode above the eye.

In actual usage, the viewer finds it easier to rotate his head and keep his eyes fixed on the object or cursor, rather than keeping his head still and moving his eyes to

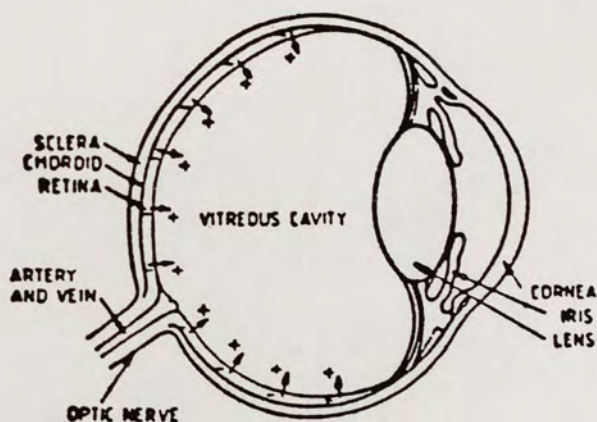


Figure 1. Static Corneo-Retinal Potential.

the direction he wants the object/cursor to go. This fact, however, does not diminish the effectiveness of the passive oculometer since the CRP measurement is made relative to the head.

Electrodes are used to collect the charge deposited on the skin by the corneo-retinal potential. Silver-silver chloride electrodes are chosen in this study, as in previous studies at the University of Central Florida. They are some of the most popular physiological electrodes because they are stable, relatively noise free, and have a low half-cell potential (Panayiotou 1984). The skin, acting as the electrolyte, is rich in chlorine ions. The silver in the electrode is oxidized where the current enters the wire. The resulting silver ions combine with the chlorine ions to form silver chloride ( $\text{AgCl}$ ), which is left on the electrode. The viewer may enhance the reaction by cleaning the skin with alcohol and applying Redux creme to the electrode.

The electrodes are attached to a ski mask that has the plastic shield removed. The mask presses the electrodes against the skin, providing better skin contact. Figure 2 illustrates the placement of the electrodes on the face and on the mask. Note that there are more electrodes for

vertical motion detection; in practice, it was observed that vertical motion is not as easily recorded as horizontal motion. Therefore, four electrodes are used to detect vertical motion, two electrodes each for above and below the eyes.

All oculometers studied at UCF have used the corneo-retinal potential as a means of measuring eye movement. Chrysanthos Panayiotou (1984) studied the feasibility of CRP in accurate measurement by designing an evaluation system. Robert Solomon (1985) measured the optimum input impedance required for an electro-oculometer. Paul Godfrey (1985) tested his electro-oculometer by asking a quadriplegic to play video games using only the oculometer as the joystick. The subject confirmed that the electro-

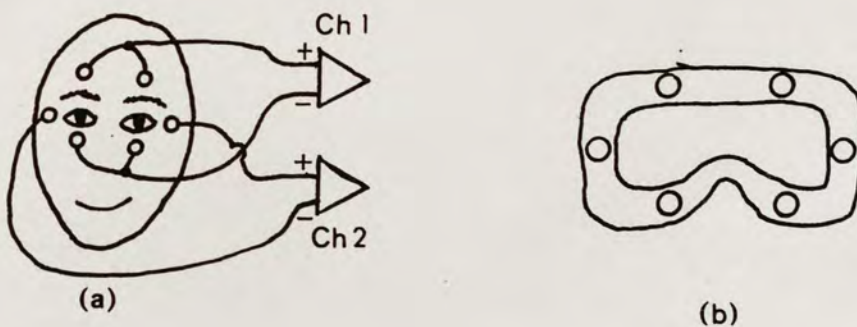


Figure 2. Placement of Electrodes (a) on the face and (b) on the ski mask.

oculometer worked well for games that did not require fine control.

The oculometer discussed in this thesis contains four stages: an instrumentation amplifier, a bandpass filter, a supplemental gain stage, and a computer interface circuit. A basic block diagram is shown in Figure 3.

The instrumentation amplifier provides gain and a means of differencing the two input signals. A circuit with high common mode rejection ratio is desired to eliminate signals common to both inputs, such as power line interference and physiological signals. Any signals that are different between the two inputs are amplified.

The bandpass stage is one of two features that set this oculometer apart from its predecessors. In Godfrey's design (1985) and Solomon's design (1985), only lowpass filtering was used, and low frequency noise was a problem.

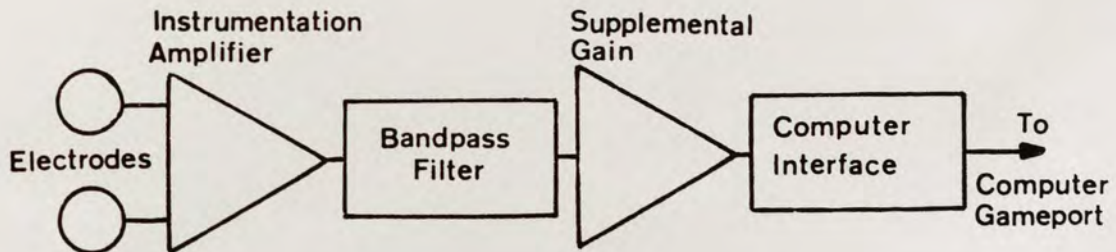


Figure 3. Basic Block Diagram of Bandpass Oculometer.

By filtering out all frequencies except where eye movement occurs, low frequency drift, as well as higher frequency interference signals, is eliminated. The result is more accuracy and smoother tracking than was previously reported in UCF oculometers.

The supplemental gain stage supplies another 50 v/v gain. A distribution of gain is desired to prevent any possible saturation of the electronics.

The computer interface stage contains the second feature that makes the bandpass oculometer unique. An optocoupler is biased to provide the same response as a joystick. This approach requires less components than Godfrey's design (1985), which was also plugged directly into the gameport of the computer. The optocoupler also provides the added safety benefit of electrically isolating the viewer from the computer.

Specifications of the complete system will be presented first. Design of each individual stage will follow. Performance of the stages will be analyzed using basic laboratory techniques, while the complete system will be tested, as Godfrey did, by using it as a joystick to play video games. Conclusions based on the results and discussion of possible improvements will complete this thesis.

## SPECIFICATIONS

In order to design a bandpass oculometer, certain specifications have to be met. The design must be safe, easy to operate, accurate in its eye tracking ability, and inexpensive in initial and operative costs. In order to fulfill these needs, an analysis of the physical phenomena involved is necessary and will be discussed in the following section.

The average field of view determines the amount of charge produced by CRP; as stated by Panayiotou (1984), this is approximately 10 uv/degree look angle. As shown in Figure 4, the average person can move his eyes 60 degrees abduction (left or right from center), 60 degrees depression (down from center), and 50 degrees elevation (up from center). Since these are extreme look angles, and a computer screen will be used, the design only needs to track up to 50 degrees abduction and depression, and to 40 degrees elevation. Therefore, the input voltage will be approximately 0.5 mv for abduction and depression, and 0.4 mv for elevation.

Amplification is necessary due to the small input voltage. A minimum gain of 80 dB or 10,000 v/v would



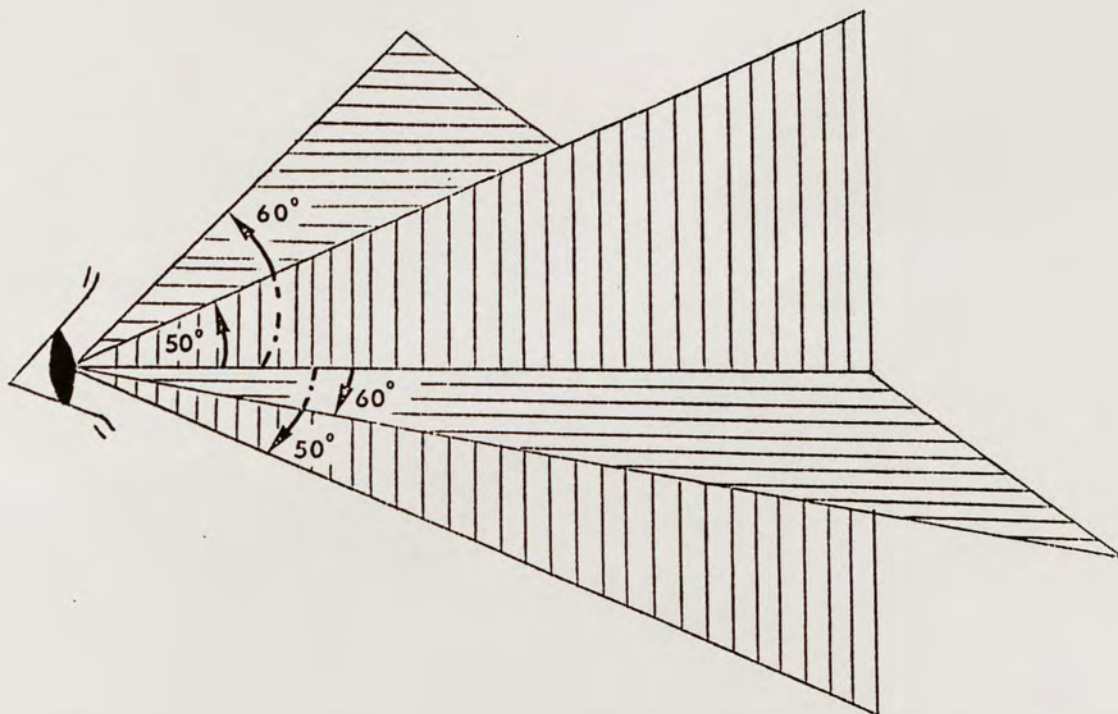


Figure 4. Average Extreme Eye Motion Angles.

provide a more sizable voltage of 4 to 5 volts. A distribution of gain is desired in order to prevent saturation of the electronics due to possible electrical surges. Therefore, the first stage gain is 200 v/v, and the supplementary gain stage will have 50 v/v.

An important consideration in any electronic circuit is noise. Flicker noise, also known as  $1/f$  noise or low frequency drift noise, is present in all active devices in the low frequency spectrum near DC voltage (Gray and Meyer

1984). Flicker noise is caused by imperfections in the crystal patterns of active devices and is associated with direct current flow. The spectral density is governed by the following equation:

$$i^2 = K_1 \left( \frac{I^a}{f^b} \right) df \quad (1)$$

where:  $df$  is a small bandwidth at frequency  $f$   
 $I$  is a direct current  
 $K_1$  is a constant for a particular device  
 $a$  is a constant between 0.5 and 2  
 $b$  is a constant of approximately 1

Note the dependence of  $1/f$  if  $b=1$ , hence the name "1/f noise." Because only lowpass filtering was used in previous studies at UCF, flicker noise was a major problem. By adjusting the lower frequency corner, DC voltage and 1/f noise can be filtered out or eliminated, as shown in the general diagram of Figure 5.

Since the only frequency spectrum of interest is where

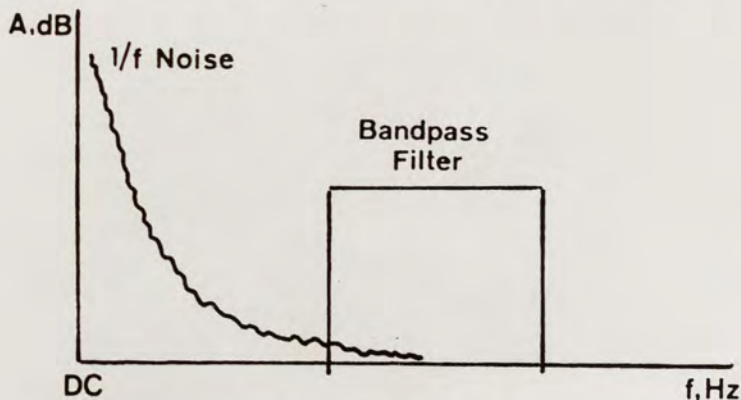


Figure 5. Low Frequency Spectrum.

eye movement occurs, a bandpass filter is proposed. Tracking eye movement is approximately 0.1 to 1 seconds in length. Consider the time it takes to move the eyes from left to right, or up and down; one second is quite a long period of time, while a "quick jump" may only take one-tenth of a second. The eye is also capable of making very fast movements called saccadic movements (Yarbus 1967). This movement is characteristic of how the eye searches for a target. Once the target is found, the eye changes to smooth tracking motion (Yarbus 1967). The designer must decide whether saccadic motion, or higher frequency motion, should be followed. Possible higher frequency interference is uncontrollable head motion due to a disease, such as cerebral palsy or Parkinson's disease. These facts determine where the upper frequency corner is set. For

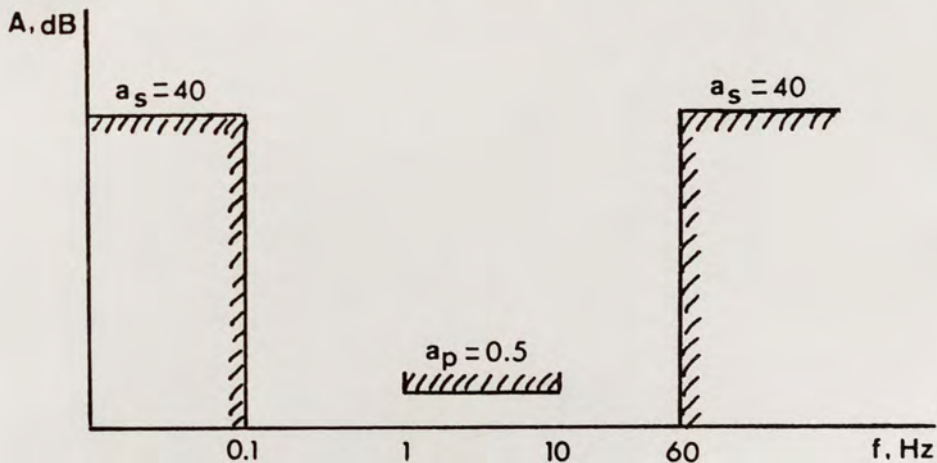


Figure 6. Stopband Configuration.

this design, the minimum and maximum loss values,  $a_s$  and  $a_p$ , respectively, were chosen as shown in the stopband configuration of Figure 6. The 0.5 dB bandwidth of 1 to 10 Hz was chosen since the rate of most eye movement falls within the range of 0.1 to 1 seconds. This bandwidth does not include very fast eye motion frequencies (i.e., saccadic) and thus will prevent unwanted movements from interfering with smooth pursuit of the object. The minimum loss,  $a_s = 40$  dB, eliminates any unwanted signal, while maximum loss,  $a_p = 0.5$  dB, passes the entire bandwidth with minimal attenuation.

The original goal in this study, and previous studies in oculometry at UCF, is to design a circuit that will allow a person to control a computer using eye/head motion exclusively. The chosen means of accessing the computer is through the gameport; this is the most convenient method of access since all personal computers have a gameport. The task then is to design a final stage that will simulate the response of a joystick.

The gameport circuitry determines joystick position by measuring how long it takes an internal capacitor to charge up to 3.15 volts (Godfrey 1985). When the capacitor reaches 3.15 volts, or 0.63 times (one RC time constant) the computer supply voltage of 5 volts, an internal transistor shorts

out the capacitor to ground (Godfrey 1985). The voltage across the capacitor can be expressed as:

$$v_c(t) = V_s(1 - e^{-t/RC}) \quad (2)$$

where  $V_s$  is the computer supply voltage,  $R$  is the joystick resistance ( $1 \text{ kohm} < R < 150 \text{ kohms}$  for the Apple II),  $C$  is the internal capacitor (22 nf), and  $t$  is the time required. Solving for  $t$  results in a linear relationship between  $R$  and  $t$ :

$$t = RC \ln \left( 1 + \frac{v_c(t)}{V_s} \right) \approx RC \ln k \quad (3)$$

where  $k$  is a constant if the maximum value of  $v_c(t)$  is used. The resistor can be expressed as a voltage divided by a current:

$$t = \frac{vC}{i} \ln k \quad (4)$$

The voltage across the gameport remains relatively constant as the joystick resistance is varied (between 4.54 to 4.87 volts). Therefore, the current is viewed as the variable factor in the equation above, varying between 0.03 and 0.3 milliamps. This fact led to the suggestion of shaping the input voltage of the last stage to control the output current flowing to the computer in the same manner that the joystick resistance does.

A plot of the joystick paddle position number (ppn)

versus joystick resistance is shown in Figure 7. A computer program developed by Godfrey, called "Oculometer Test Program" or Vector Test (1985) was used. It draws a vector from the cursor position relative to the center of the computer screen and assigns a number between 0 and 255

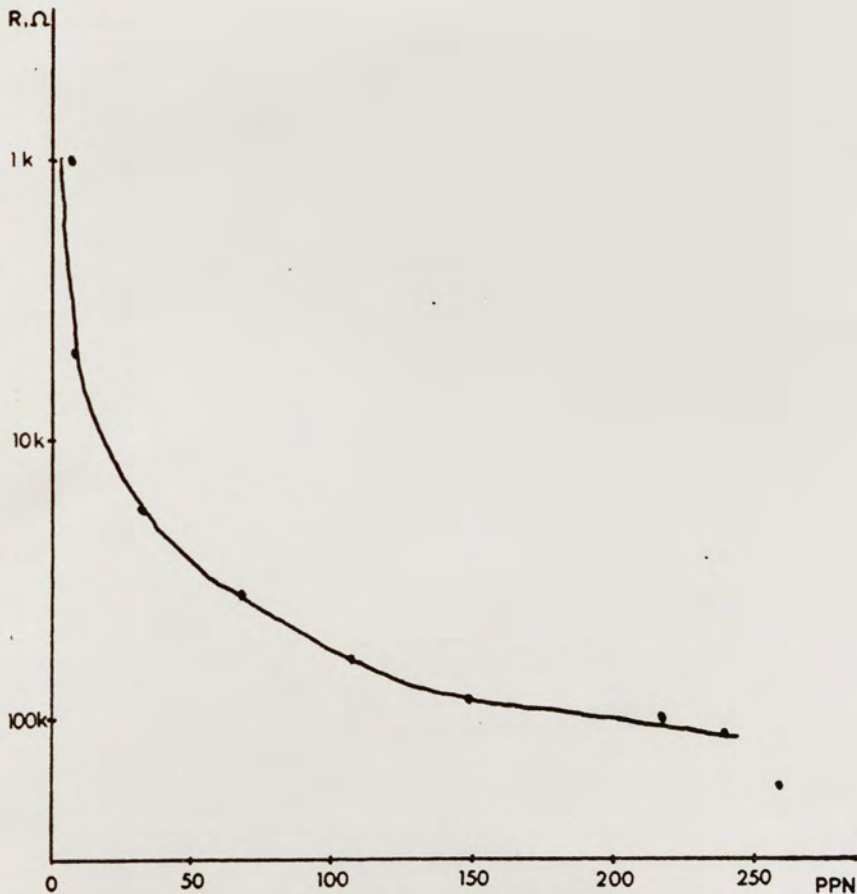


Figure 7. Paddle Position vs. Joystick Resistance.

to the horizontal and vertical position (ppn). The data points were found by placing a decade resistance box onto the gameport of the computer and increasing the resistance until a change in the ppn was noted. Note the  $1/x$  shape of the resulting plot.

A diode shaping network is used to simulate this  $1/x$  response by controlling the output current based on input voltage. The input voltage swing of this stage is + or - 5 volts; therefore, the break off voltages specified to produce a  $1/x$  shape are -4.5, -3, and 0, and the slopes required are -9, -2.5, -0.69, and -0.15.

Table 1 summarizes all specifications for the bandpass oculometer.

TABLE 1  
SUMMARY OF SPECIFICATIONS

STAGE #	SPECIFICATIONS
1	Minimum Gain: 200v/v
2	Highpass: $a_s = 40$ dB $f_s = 0.1$ Hz $a_p = 0.5$ dB $f_p = 1$ Hz Lowpass: $a_s = 40$ dB $f_s = 60$ Hz $a_p = 0.5$ dB $f_p = 10$ Hz
3	Minimum Gain: 50 v/v
4	Break off voltages: -4.5, -3, and 0 Slopes: -9, -2.5, -0.69, and -0.15

## SYSTEM DESIGN

The following section describes the circuits designed to meet the specifications.

### Instrumentation Amplifier

The purpose of this first stage is two-fold: first, it will filter out any signals that are common to the two inputs or electrodes; second, it will amplify by 200 v/v (contributing to the overall system gain of 10,000 v/v) any signals that are different between the two inputs. Circuits that provide high common mode rejection ratio (CMRR) are typically used for this task. (For a brief explanation of CMRR, refer to Appendix A.)

The circuit chosen for its high CMRR is the classic three instrumentation amplifier, shown in Figure 8. The input is shunted with 47 kilohm resistors ( $R_8$  and  $R_9$ ) to provide the optimum input impedance (Solomon 1985). The CMRR for this circuit is derived in Appendix B. The differential gain was found to be:

$$A_d = - \frac{R_5}{R_4} \left( 1 + 2 \frac{R_1}{R_2} \right) \quad (5)$$

where  $R_1$ ,  $R_4$ , and  $R_5$  are fixed and  $R_1=R_3$ ,  $R_4=R_6$ , and  $R_5=R_7$ .



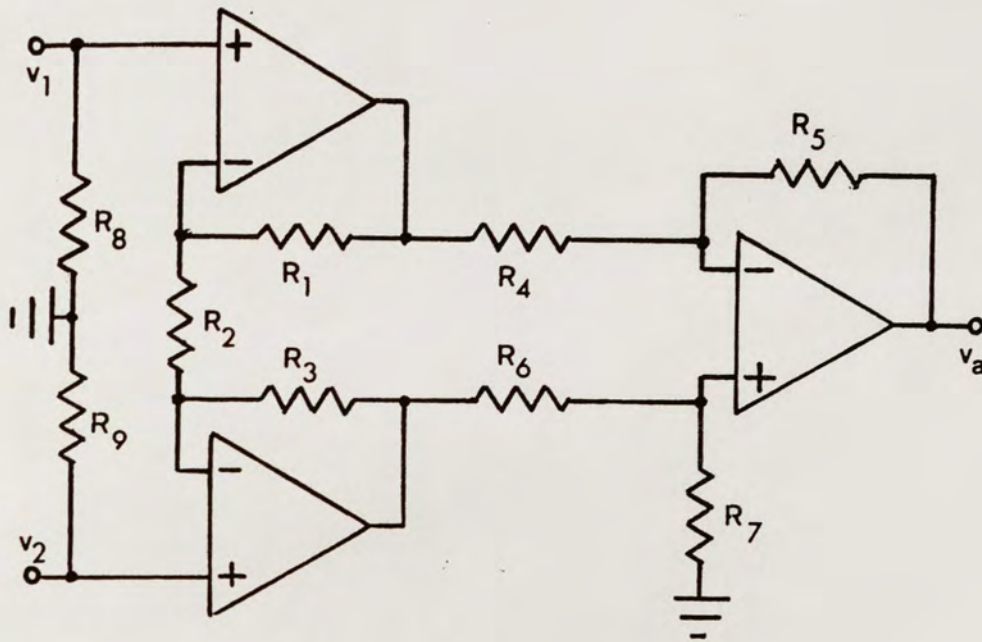


Figure 8. Classic Three Instrumentation Amplifier.

Under these assumptions, it is critical that the resistor pairs are matched precisely; then,  $R_2$  alone controls the differential gain.

Table 2 provides nominal and measured resistor values used in this study. From the nominal values, the expected differential gain is  $-204.7$  v/v.

#### Bandpass Filter

The second stage of the oculometer is a bandpass filter; it is not a conventional bandpass filter, but a

TABLE 2

## RESISTOR VALUES FOR INSTRUMENTATION AMPLIFIER

<u>RESISTOR</u>	<u>NOMINAL</u>	<u>MEASURED #1</u>	<u>MEASURED #2</u>
R <sub>1</sub>	100k	99.1k	98.75k
R <sub>2</sub>	4.7k	4.709k	4.705k
R <sub>3</sub>	100k	99.1k	98.67k
R <sub>4</sub>	10k	9.983k	10.00k
R <sub>5</sub>	47k	46.8k	47.1k
R <sub>6</sub>	10k	9.985k	9.997k
R <sub>7</sub>	47k	46.8k	46.98k
R <sub>8</sub>	47k	46.9k	46.93k
R <sub>9</sub>	47k	46.9k	46.93k

Note: All resistors are in ohms.

lowpass and a highpass filter in cascade. This cascade design is necessary due to low quality factor. Quality factor,  $Q$ , is the ratio of reactance at frequency  $\omega_0$  to resistance (Van Valkenburg 1982); it also can be expressed in terms of center frequency and -3 dB bandwidth as:

$$Q = f_0/BW \quad (6)$$

Usually, a bandpass filter such as the Delyiannis-Friend circuit would be used; however, the following equation must be satisfied (Van Valkenburg 1982):

$$H = \frac{1}{2Q^2} \quad (7)$$

For a unity gain, the  $Q$  must be  $(0.5)^{1/2}$  or 0.7071. The

specifications given earlier suggest a center frequency of approximately 3.1623 Hz and a -3 dB bandwidth of 14.8 Hz. This results in a Q of 0.2137, which is too low.

A Butterworth-type filter was chosen for its maximally flat passband and its ease in design. It utilizes Sallen and Key lowpass and highpass networks (Figure 9). The design procedure, in Appendix C, analyzes the stopband configuration (refer to Figure 6) to determine the number of poles needed to satisfy  $a_{\min}$  and  $a_{\max}$ . This design also has the added benefit of providing a range of capacitor values that will satisfy the specifications; this enables the designer to choose the more readily available 10% tolerance values rather than depend on the availability of odd-value capacitors.

The general transfer function for a two-pole lowpass stage, as shown in Figure 9, is:

$$T(s) = \frac{1}{\frac{s^2}{\omega_o^2} + \frac{s}{\omega_o}(2 \cos Y_o) + 1} \quad (8)$$

where  $Y_o$  is the corresponding Butterworth angle. As shown in Appendix C, the design procedure determined that four poles, or two second order stages, were necessary for the lowpass and highpass each. The final design is shown in

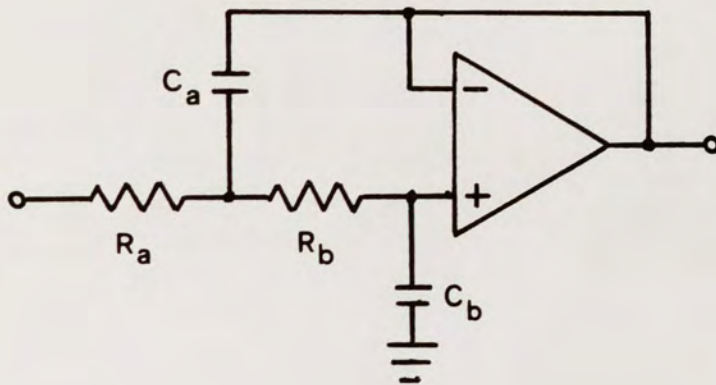


Figure 9. Sallen and Key Lowpass Circuit (Second Order).

Figure 10. The nominal and measured values of the components are shown in Table 3.

TABLE 3

COMPONENT VALUES FOR BANDPASS STAGE

<u>COMPONENT</u>	<u>NOMINAL</u>	<u>MEASURED #1</u>	<u>MEASURED #2</u>
R <sub>10</sub>	240k	246.6k	249.6k
R <sub>11</sub>	27k	28.75k	28.69k
R <sub>12</sub>	330k	348.4k	328.4k
R <sub>13</sub>	30k	31.02k	32.54k
R <sub>14</sub>	750k	774.1k	752.5k
R <sub>15</sub>	820k	837.2k	837.2k
R <sub>16</sub>	300k	325.5k	317.0k
R <sub>17</sub>	2M	1.9896M	1.9994M
C <sub>1</sub>	0.22u	0.228u	0.208u
C <sub>2</sub>	68n	69.8n	66.7n
C <sub>3</sub>	0.47u	0.475u	0.476u
C <sub>4</sub>	22n	22.7n	21.9n
C <sub>5</sub>	1u	1.099u	0.995u
C <sub>6</sub>	1u	1.036u	0.947u
C <sub>7</sub>	1u	1.074u	0.997u
C <sub>8</sub>	1u	1.040u	0.987u

Note: All resistors are in ohms, and all capacitors are in farads.

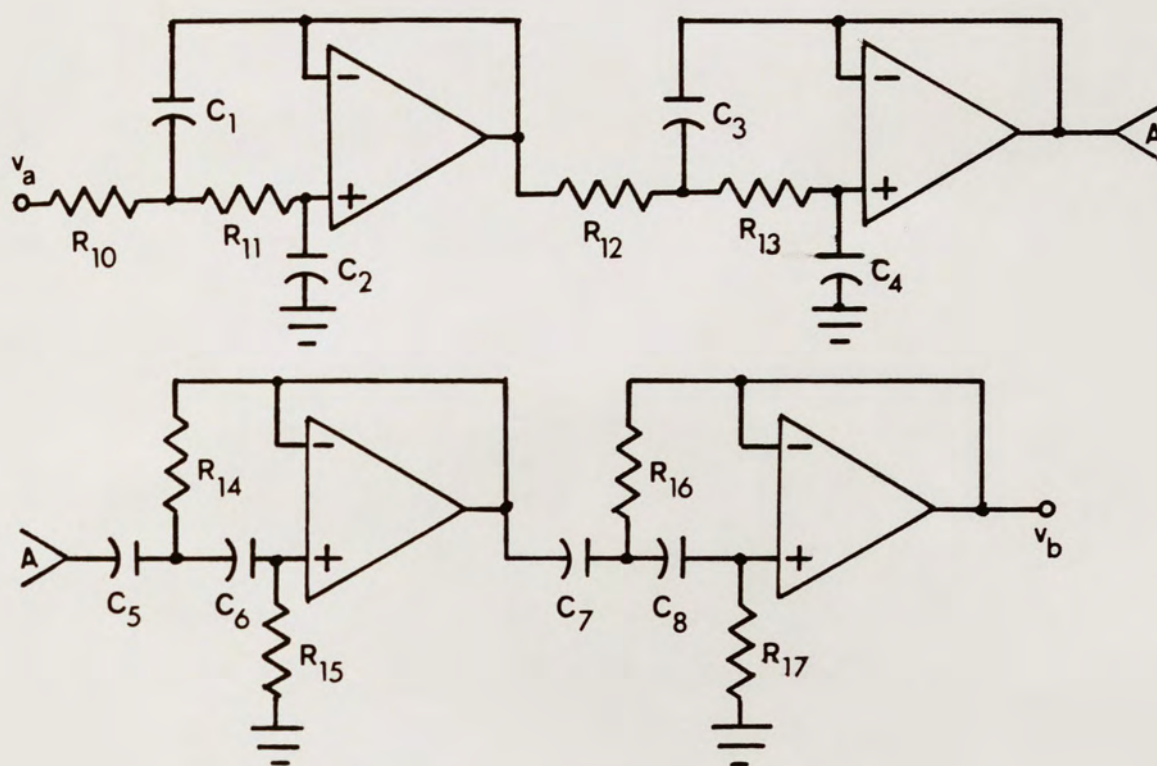


Figure 10. Bandpass Filter.

#### Supplemental Gain

The supplemental gain stage provides another 50 v/v of gain to increase the overall gain to 10,000 v/v. Two basic inverting networks are utilized, one with a gain of 10 v/v and one with a gain of 5 v/v. They are cascaded together as shown in Figure 11. Table 4 gives both nominal and measured resistor values.

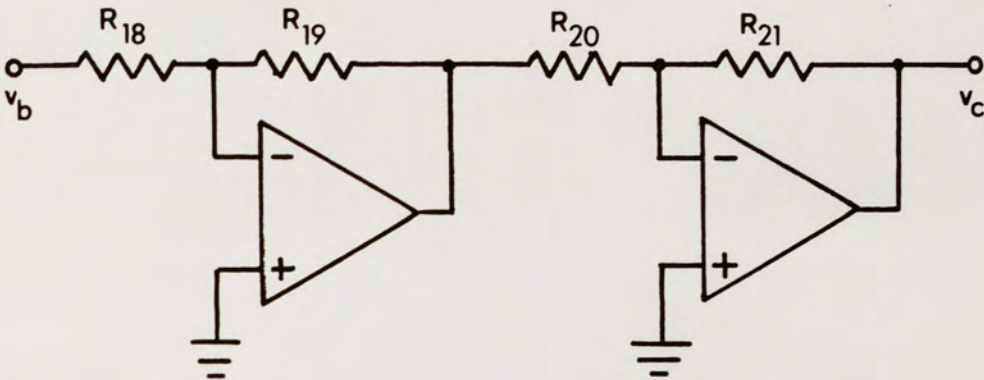


Figure 11. Supplemental Gain Stage.

TABLE 4

RESISTOR VALUES FOR SUPPLEMENTAL GAIN

<u>RESISTOR</u>	<u>NOMINAL</u>	<u>MEASURED #1</u>	<u>MEASURED #2</u>
R <sub>18</sub>	10k	10.014k	9.960k
R <sub>19</sub>	100k	99.26k	98.20k
R <sub>20</sub>	10k	10.003k	9.992k
R <sub>21</sub>	51k	49.93k	49.94k

Note: All resistors are in ohms.

### Computer Interface

The final stage of the bandpass oculometer is the computer interface stage. This stage must duplicate the response of a joystick such that the oculometer can be plugged directly into the gameport of a computer.

The response of a joystick was measured and plotted,

as illustrated in Figure 7 of the specifications. From this plot, it was determined that a diode shaping network with a  $1/x$  response would work well.

The diode shaping network in Figure 12 was used. In order to illustrate how this circuit works, a simpler version, as shown in Figure 13, will be discussed. This circuit only has one break point and two slopes.

The slopes are set in the following manner. From the maximum positive swing to the break off voltage chosen, the diode is not conducting. Therefore, the circuit is a basic inverter with a slope of  $-R_3/R_1$ . From the break off voltage to the maximum negative swing, the diode is conducting. The slope is then regulated by the combined resistor ratios of  $-(R_3/R_1)-(R_3/R_B)$ . Once  $R_3$  is chosen, any slopes can be created by varying  $R_1$  and  $R_B$ .

To find what resistors control the break off voltage, the following approach is used. The virtual ground at the inverting terminal of the op amp results in the diode network shown in Figure 14. By Kirchoff's current laws, it is found that:

$$\frac{15 + V_D}{R_A} = \frac{V_{in} + V_D}{R_B}$$

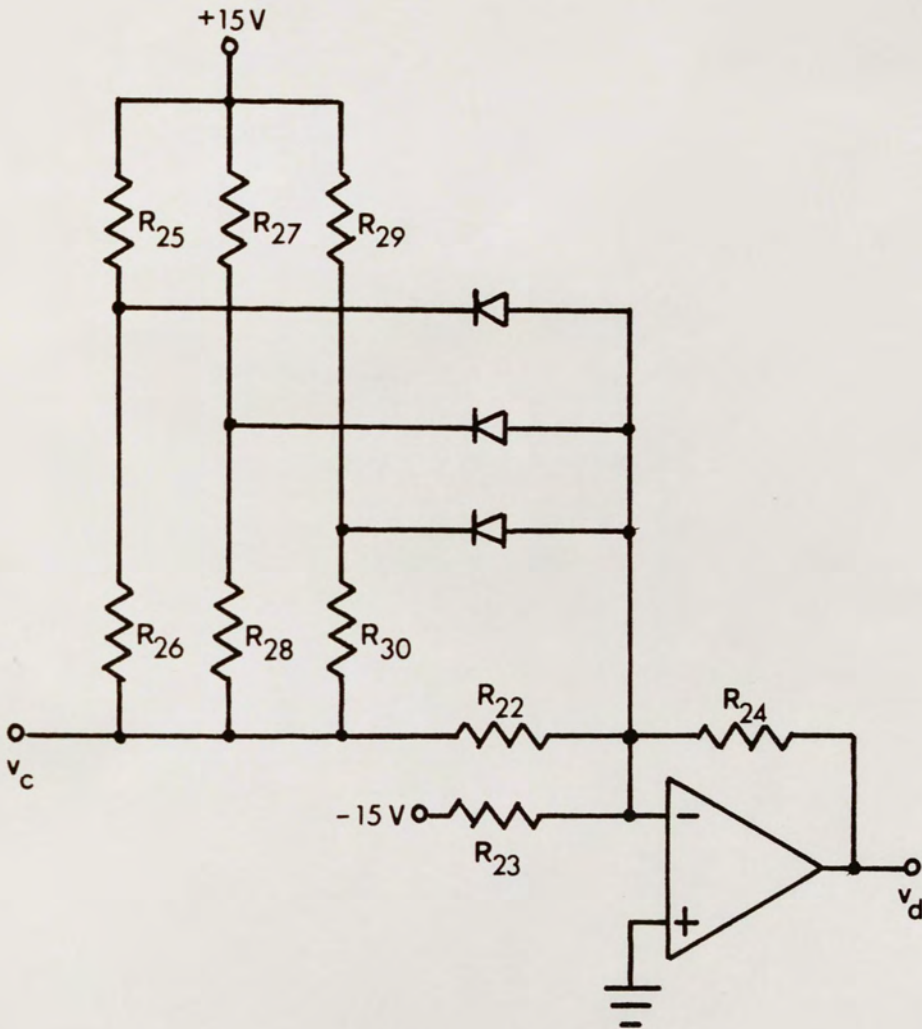


Figure 12. Diode Shaping Network.



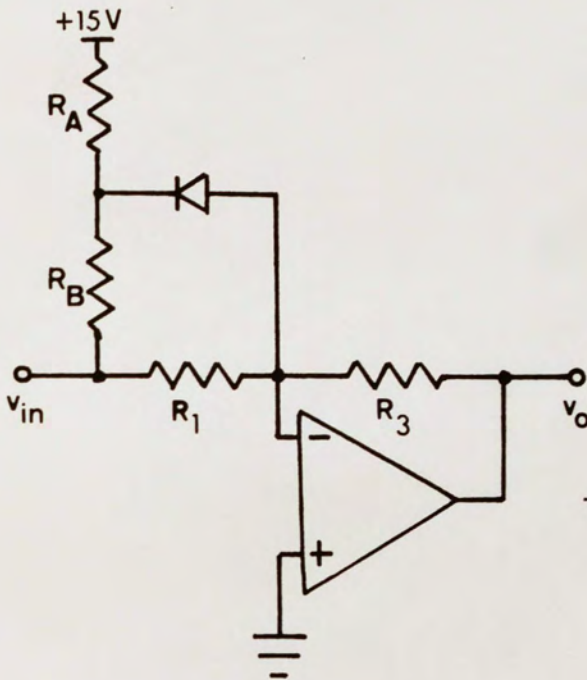


Figure 13. Simpler Version of Diode Shaping Network.

where  $v_D$  is the diode voltage (approximately 0.7 volts) and  $v_{in}$  is the input voltage. Let  $v_{in} = v_C$  (the break off voltage desired); the corresponding resistor values can be

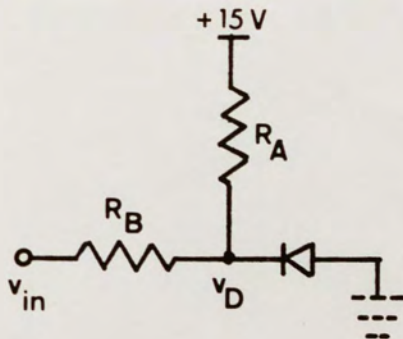


Figure 14. Break Off Voltage Circuitry.

computed from:

$$\frac{R_B}{R_A} = \frac{|v_C| + v_D}{15 + v_D} = \frac{|v_C| + 0.7}{15.7}$$

where  $R_B$  is set by the slope desired.

Referring back to Figure 12, the chosen break off voltages at 0, -3, and -4.5 volts are controlled by the resistor ratios of  $R_{26}/R_{25}$ ,  $R_{28}/R_{27}$ , and  $R_{30}/R_{29}$ , respectively. The slopes between each break off voltage are controlled by the resistor ratios listed in Table 5. The proper bias is provided by a 100 kohm potentiometer,  $R_{23}$ , and the -15 volt supply voltage. The potentiometer allows

TABLE 5

PARAMETERS THAT CONTROL SLOPE OF SHAPING NETWORK

<u>INPUT VOLTAGE RANGE</u>	<u>RESISTORS</u>						
-5 to -4.5	$\frac{R_{24}}{R_{22}}$	$+$	$\frac{R_{24}}{R_{26}}$	$+$	$\frac{R_{24}}{R_{28}}$	$+$	$\frac{R_{24}}{R_{30}}$
-4.5 to -3	$\frac{R_{24}}{R_{22}}$	$+$	$\frac{R_{24}}{R_{26}}$	$+$	$\frac{R_{24}}{R_{28}}$		
-3 to 0	$\frac{R_{24}}{R_{22}}$	$+$	$\frac{R_{24}}{R_{26}}$				
0 to 5				$\frac{R_{24}}{R_{22}}$			

the viewer to adjust the bias for optimum performance.

An optocoupler (4N35) was chosen as the link between the diode shaping network and the computer. An operational amplifier with the optocoupler in the feedback (Figure 15) was cascaded to the shaping network. The inverting resistor,  $R_{31}$ , controls the amount of current that flows into the optocoupler. Using a maximum voltage of 5 volts and a maximum current of 0.3 milliamps, 16.67 kohms is calculated, but the nominal value of 15 kohms is used. The computer supply voltage of +5 volts is connected to the collector of the phototransistor, while the emitter is connected directly to the gameport like a joystick.

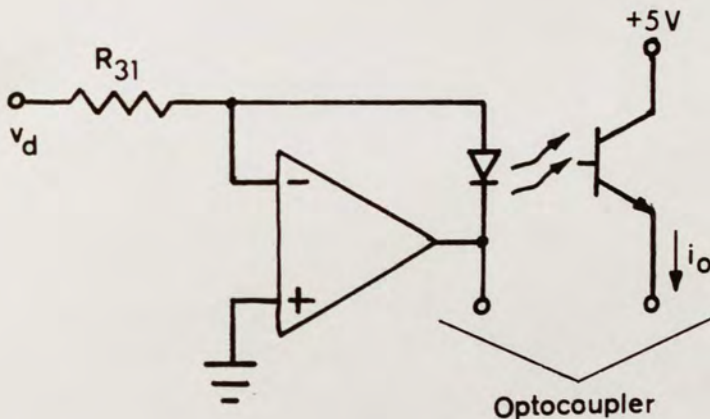


Figure 15. Optocoupler Network.

Table 6 lists nominal and measured resistor values for this design.

TABLE 6  
RESISTOR VALUES FOR COMPUTER INTERFACE

<u>RESISTOR</u>	<u>NOMINAL</u>	<u>MEASURED #1</u>	<u>MEASURED #2</u>
R <sub>22</sub>	68k	65.72k	67.10k
R <sub>23</sub>	100k	100.20k	100.22k
R <sub>24</sub>	10k	9.998k	10.005k
R <sub>25</sub>	430k	448.7k	439.2k
R <sub>26</sub>	18k	17.712k	18.351k
R <sub>27</sub>	24k	24.07k	23.87k
R <sub>28</sub>	5.6k	5.845k	5.547k
R <sub>29</sub>	4.3k	4.351k	4.383k
R <sub>30</sub>	1.5k	1.5022k	1.5012k
R <sub>31</sub>	15k	14.981k	15.027k

Note: All resistors are in ohms.

## RESULTS

As the bandpass oculometer was built, each stage was tested, and its performance analyzed. The following section will outline the procedures used. Recall that two identical channels were built: one each for horizontal and vertical.

### Instrumentation Amplifier

Common mode rejection ratio was the only test for the first stage, the instrumentation amplifier. As outlined in Appendix A, the differential mode and common mode gains were measured. Table 7 provides the results for each channel. A sinusoid with a frequency of 40 Hz was used as the voltage source. This was the lowest frequency possible for legible measurements.

Recalling Table 2, it is once again emphasized that well matched resistors, as in channel #1, improves CMRR. The lower CMRR in channel #2 is not a disadvantage, however. As stated previously, in practice it was observed that horizontal eye movement is more easily recorded. Therefore, in order to "even out" the response between horizontal and vertical, channel #1 was chosen to measure

TABLE 7  
COMMON MODE REJECTION RATIO FOR  
INSTRUMENTATION AMPLIFIER

	<u>A<sub>d</sub></u>	<u>A<sub>c</sub></u>	<u>CMRR</u>
channel #1	50.0	0.0020	87.96 dB
channel #2	50.0	0.0044	81.11 dB

vertical motion.

Since the differential mode signal is more than 10,000 times greater than the common mode signal, the CMRR for each channel was deemed satisfactory.

#### Bandpass Filter

For the bandpass filter stage, an AC frequency response was run on Microcap 4.1, a microcomputer circuit analysis program (Spectrum Software 1983). Microcap verified that the design met the specifications before the circuit was built. The Microcap results are shown in Figure 16.

After the bandpass filter was built, an HP 3582A spectrum analyzer was used to run an ac frequency response. Photographs were taken directly from the spectrum analyzer using a scope camera. Figures 17 and 18 are photographs from channel 1, while Figures 19 and 20 are from channel 2.

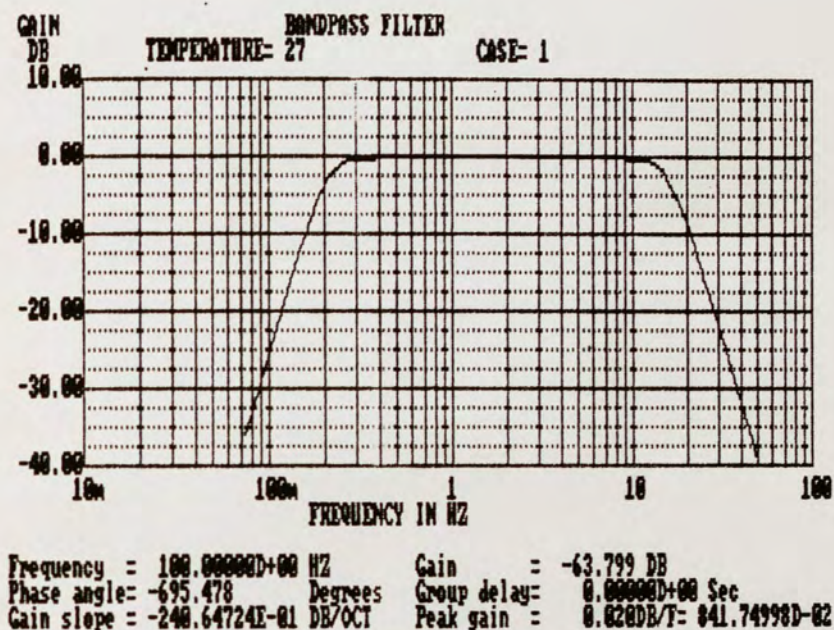


Figure 16. Microcap AC Analysis Results.

Note that the -3 dB frequency is displayed. Sixty-four data points were used by the spectrum analyzer to compile these plots; the data points are listed in Appendix D.

As one can see from the data, the specifications were met.

The first two stages were then tested together by connecting electrodes at the inputs and an oscilloscope at the output. Using the x-y mode on the oscilloscope, where x is connected to horizontal and y is connected to vertical, the subject could move the "dot" on the screen by moving her head relative to her eyes. Once again, it was

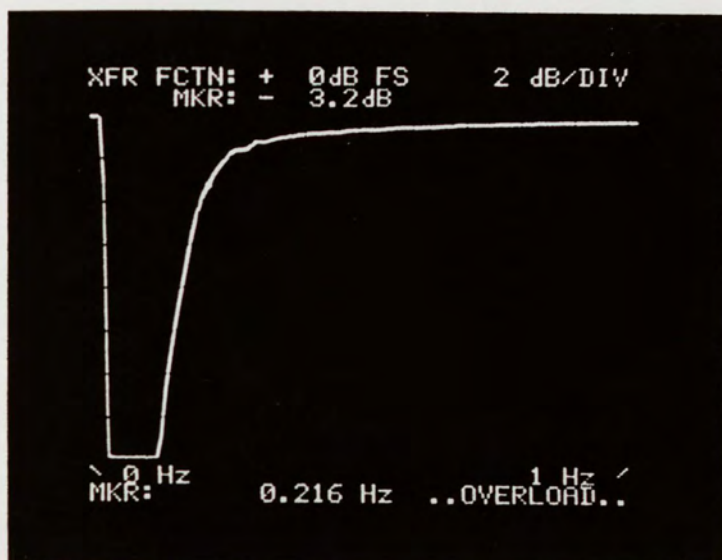


Figure 17. Frequency Response of Channel 1 (0-1 Hz).



Figure 18. Frequency Response for Channel 1 (0-25 Hz).



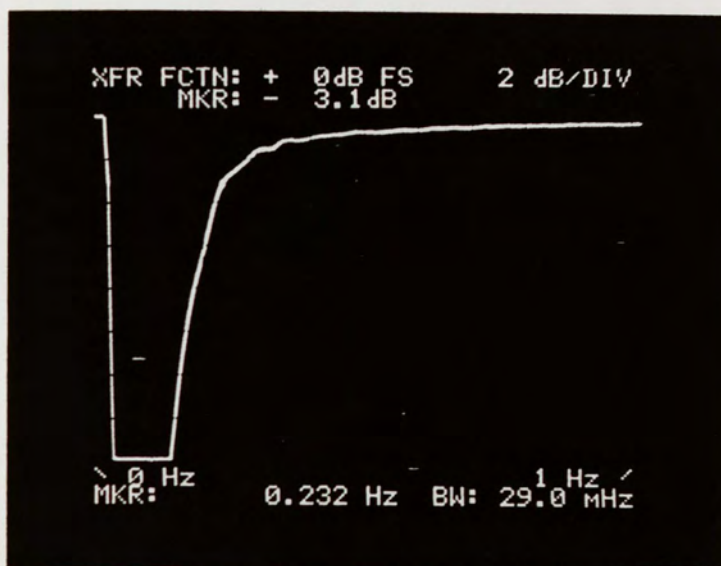


Figure 19. Frequency Response for Channel 2 (0-1 Hz).



Figure 20. Frequency Response for Channel 2 (0-25 Hz).

noted that horizontal movement was more accurately traced in comparison to vertical movement. However, the performance was acceptable despite the slight difference between the channels.

#### Supplemental Gain

The supplemental gain stage was tested by simple gain measurements. Table 8 lists the measured data. These data confirm that the specifications are met.

TABLE 8

MEASUREMENTS FOR SUPPLEMENTAL GAIN

	<u>V<sub>in</sub></u>	<u>V<sub>o</sub></u>	<u>Gain</u>
Channel 1	0.2	11	55
Channel 2	0.2	10.5	52.5

Note: The voltages shown are amplitudes of a sinusoid input source with a frequency of 40 Hz.

#### Computer Interface

The first test for the computer interface was to see if the transfer of output current versus input voltage had the 1/x shape. A 1 kohm resistor was shunted across the output of the diode shaping network in order to measure an output voltage. A photograph of the transfer function was taken using a scope camera (Figure 21), and one can see

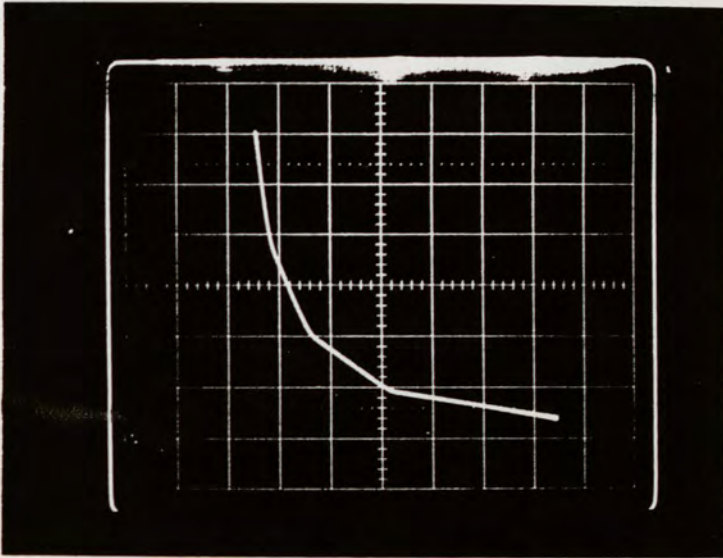


Figure 21. Transfer Response of the Diode Shaping Network.

that the  $1/x$  response is duplicated.

#### System Test

The last, and ultimate, test for this circuit was to connect the completed network to the Apple IIc computer and run the Vector Test program. After approximately fifteen minutes, the electrodes and system are stabilized, and the oculometer is ready for evaluation.

The oculometer traced all eye motion made in a deliberate manner. The viewer can trace any simple figure, with a minimal amount of practice, by moving his head

relative to his eyes.

In his results, Godfrey explained that the formation of a dot by staring at the center of the screen was rarely possible due to the offset created by accumulated drift noise in his system (1985). Furthermore, it was noted after publication that the offset caused the cursor to drift to the edge of the field of view within 30 seconds. To compensate for this offset, he employed a feedback network that would compare the position voltage to the voltage at the edge of the field of view. This provided the user a means of eliminating the offset voltage by looking quickly to the edge of the screen, then back to the center. While the offset was dealt with, it was not eliminated. Since this design utilizes bandpass filtering, the drift is eliminated, making the formation of the dot possible. If the viewer is looking directly at the center, the vector becomes a dot and remains a dot. This is a significant improvement from previous oculometers.

While the oculometer worked quite well on the Vector Test program, it did not work as well on the other computer games. It was difficult to keep the object in the game going in one direction for any length of time. This is the result of the low frequency corner (governed by the high-pass filter) being too high and thus filtering out neces-

sary eye movements. However, this difficulty can be easily rectified by simple design changes which will be discussed in the conclusions.

## CONCLUSIONS AND RECOMMENDATIONS

The main objective of this thesis was to improve the performance of the oculometer. The bandpass filtering eliminated the drift noise that plagued earlier studies. A direct consequence of using a bandpass filter is the natural tendency for the cursor to settle at the center of the screen. This type of response is ideal for an automatic firing system, where the pilot would simply align the enemy within the cross-hairs of his field of view; the "cursor" would settle in the center, and the system would fire.

For the application of using the computer for word processing or video games, the following improvements are recommended. To lower the highpass cut-off frequency, the highpass filter capacitors can be changed from 1 uf to 3 uf. This changes the cut-off frequency from 0.2027 Hz to 0.06758 Hz. The frequency corner can be lowered as needed, as long as the low frequency drift noise remains out of the passband. If the presence of DC voltage as a reference is needed for optimum performance, then an oculometer that combines bandpass filtering and an added DC voltage needs to be developed. This would provide the needed reference, as well as the 1/f noise filtering.

A similar design that runs on the computer's voltage supply of 5 volts (available through the gameport) or on batteries could be produced. This would allow the oculometer to be independent of any external voltage supplies, resulting in a more economical, and safer, system for the user.

Another interface can be designed to simulate the response of a mouse. Many new programs, especially word processing programs, use a mouse to control the computer.

APPENDIX A

COMMON MODE REJECTION RATIO



## APPENDIX A

Common mode rejection ratio is a measure of how well a circuit can eliminate common signals and amplify different signals between two input voltages. The fundamental equation is:

$$v_o = A_d(v_1 - v_2) + A_c(v_1 + v_2)/2 \quad (11)$$

Two measurements are made.

The first measurement is common mode gain ( $A_c$ ), which is found by driving the same voltage source into both inputs (see Figure 22). Since  $v_1 = v_2$ , there is no difference signal, and the fundamental equation reduces to:

$$v_o = A_c(2v_1)/2 = A_c v_1 \quad (12)$$

or

$$A_c = v_o/v_1 \quad (13)$$

For high CMRR,  $A_c$  should be very small; ideally, it is zero.

The second measurement is difference mode gain ( $A_d$ ). As one signal is fed into one input, the other input receives the same signal, but 180 degrees out of phase (see Figure 23). Since  $v_1 = -v_2$ , the two inputs add to zero at any point in time. Therefore, there is no common signal, and the fundamental equation reduces to:

$$v_o = A_d(v_1 - (-v_1)) = 2A_d v_1 \quad (14)$$

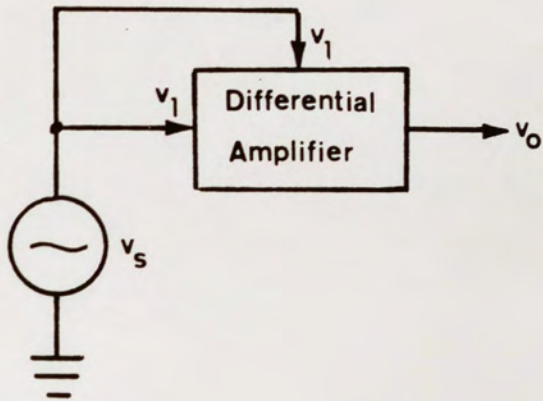


Figure 22. Measurement of Common Mode Gain.

or 
$$A_d = v_o / 2v_1 \quad (15)$$

The two measurements are used in the following equation:

$$\text{CMRR} = 20 \log (A_d / A_c) \quad (16)$$

The units are in decibels (dB). Ideally, CMRR is infinite.

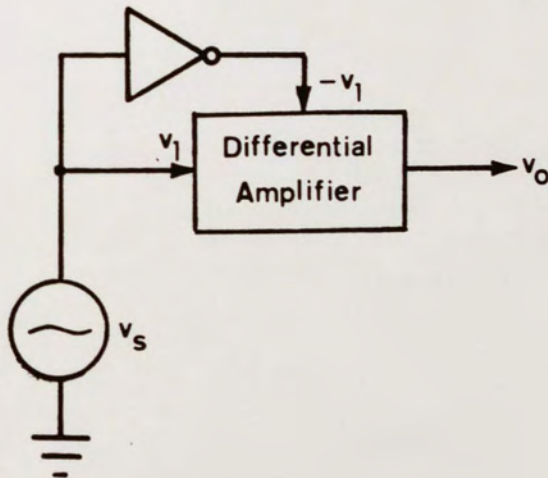


Figure 23. Measurement of Differential Mode Gain.

APPENDIX B

DERIVATION OF CMRR FOR THE  
CLASSIC THREE INSTRUMENTATION AMPLIFIER

## APPENDIX B

The classic three instrumentation amplifier is made up of two stages: a balanced line amplifier and a basic differential amplifier. Analysis is relatively easy using superposition and assuming linear operation and ideal operational amplifiers.

The overall output of the differential amplifier is:

$$v_o = - \frac{R_5}{R_4} v_{o1} + \frac{R_7}{R_6+R_7} \left( 1 + \frac{R_5}{R_4} \right) v_{o2} \quad (17)$$

The outputs to the balanced line amplifier,  $v_{o1}$  and

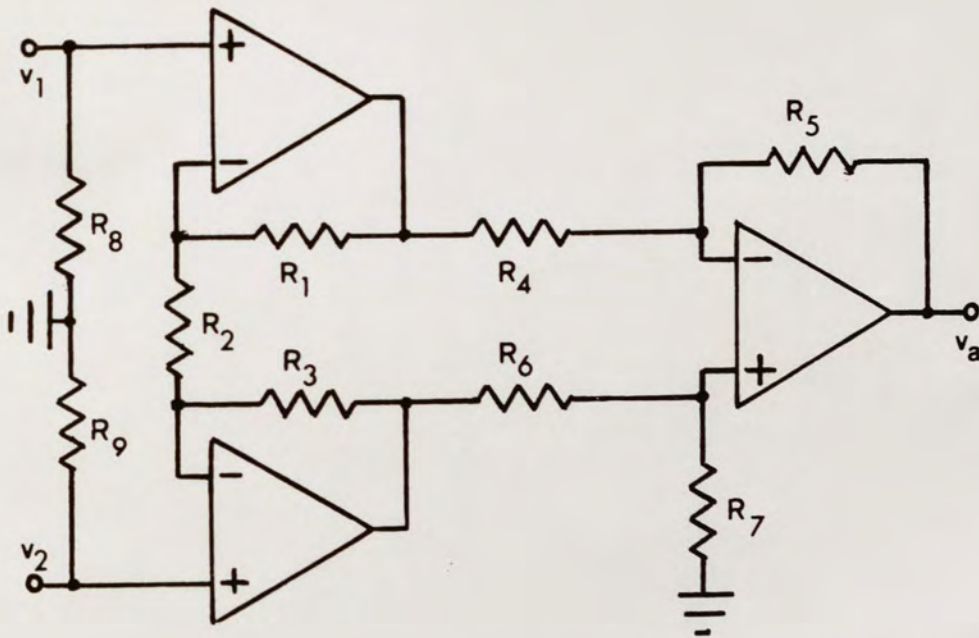


Figure 24. Classic Three Instrumentation Amplifier.

$v_{o2}$ , are:

$$v_{o1} = v_{o1a} + v_{o2b} = \left(1 + \frac{R_1}{R_2}\right)v_1 - \frac{R_1}{R_2}v_2 \quad (18)$$

$$v_{o2} = v_{o2a} + v_{o2b} = -\frac{R_3}{R_2}v_1 + \left(1 + \frac{R_3}{R_2}\right)v_2 \quad (19)$$

These equations are now plugged into equation (17) for the total response of the classic three amplifier:

$$v_o = -\frac{R_5}{R_4} \left[ \left(1 + \frac{R_1}{R_2}\right)v_1 - \frac{R_1}{R_2}v_2 \right] + \frac{R_7}{R_6+R_7} \left(1 + \frac{R_5}{R_4}\right) \left[ -\frac{R_3}{R_2}v_1 + \left(1 + \frac{R_3}{R_2}\right)v_2 \right] \quad (20)$$

Combining like terms:

$$v_o = A_1v_1 + A_2v_2 \quad (21)$$

where:

$$A_1 = -\frac{R_5}{R_4} \left(1 + \frac{R_1}{R_2}\right) - \frac{R_3}{R_2} \left(\frac{R_7}{R_6+R_7}\right) \left(1 + \frac{R_5}{R_4}\right) \quad (22)$$

$$A_2 = \frac{R_1R_5}{R_2R_4} + \frac{R_7}{R_6+R_7} \left(1 + \frac{R_5}{R_4}\right) \left(1 + \frac{R_3}{R_2}\right) \quad (23)$$

As stated in Appendix A, the fundamental equation for finding common mode rejection ratio is:

$$v_o = A_d(v_1 - v_2) + A_c(v_1 + v_2)/2 \quad (24)$$

which can also be written as:

$$v_o = [A_d + (A_c/2)]v_1 + [(A_c/2) - A_d]v_2 \quad (25)$$

Comparing this equation to equation (21), the following equalities hold:

$$A_1 = A_d + (A_c/2) \quad (26)$$

$$A_2 = (A_c/2) - A_d \quad (27)$$

Solving for  $A_d$  and  $A_c$ :

$$A_d = (A_1 - A_2)/2 \quad (28)$$

$$A_d = \frac{1}{2} \left[ - \frac{R_5}{R_4} \left( 1 + \frac{R_1}{R_2} \right) - \frac{R_3}{R_2} \left( \frac{R_7}{R_6+R_7} \right) \left( 1 + \frac{R_5}{R_4} \right) - \frac{R_1 R_5}{R_2 R_4} - \frac{R_7}{R_6+R_7} \left( 1 + \frac{R_5}{R_4} \right) \left( 1 + \frac{R_3}{R_2} \right) \right] \quad (29)$$

and 
$$A_c = A_1 + A_2 \quad (30)$$

$$A_c = - \frac{R_5}{R_4} \left( 1 + \frac{R_1}{R_2} \right) - \frac{R_3}{R_2} \left( \frac{R_7}{R_6+R_7} \right) \left( 1 + \frac{R_5}{R_4} \right) + \frac{R_1 R_5}{R_2 R_4} + \frac{R_7}{R_6+R_7} \left( 1 + \frac{R_5}{R_4} \right) \left( 1 + \frac{R_3}{R_2} \right) \quad (31)$$

For symmetry, let  $R_1=R_3$ ,  $R_4=R_6$ ,  $R_5=R_7$ ; the differential mode gain equation reduces to:

$$A_d = - \frac{R_5}{R_4} \left( 1 + 2 \frac{R_1}{R_2} \right) \quad (32)$$

and the common mode gain equation reduces to zero. Therefore, to ensure high CMRR for this amplifier, the resistors must be matched precisely to ensure  $A_c$  approaches zero.

APPENDIX C  
BANDPASS FILTER DESIGN

### APPENDIX C

To derive the Butterworth design procedure, ideal operational amplifiers are assumed. The transfer function of a Sallen and Key lowpass stage (Figure 25) is:

$$\frac{V_o(s)}{V_{in}(s)} = \frac{1}{R_1 R_2 C_1 C_2 s^2 + (R_1 + R_2) C_2 s + 1} \quad (33)$$

Equating coefficients with the standard lowpass form of equation:

$$\frac{V_o(s)}{V_{in}(s)} = \frac{1}{\frac{s^2}{\omega_c^2} + \frac{s}{\omega_c} (2 \cos Y_k) + 1} \quad (34)$$

the following design equations are produced:

$$\omega_c^2 = \frac{1}{R_1 R_2 C_1 C_2} \quad (35)$$

$$\frac{2 \cos Y_k}{\omega_c} = (R_1 + R_2) C_2 \quad (36)$$

or

$$Q_k \omega_c = \frac{1}{(R_1 + R_2) C_2} \quad (37)$$

where  $2 \cos Y_k = 1/Q_k$ ;  $Q_k$  is the quality factor and is different for each stage  $k$ . Combining equations (35)

and (36):

$$\frac{1}{Q_k} = 2 \cos Y_k = \frac{(R_1 + R_2) C_2}{(R_1 R_2 C_1 C_2)^{1/2}} \quad (38)$$



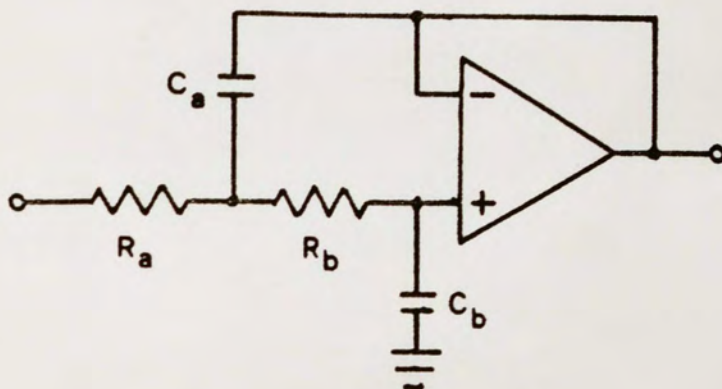


Figure 25. Sallen and Key Lowpass Stage (Second Order).

After a little manipulation, a quadratic form is achieved:

$$\frac{R_1}{R_2} + \left(\frac{R_1}{R_2}\right)^{1/2} \left[-2 \cos Y_k \left(\frac{C_1}{C_2}\right)^{1/2}\right] + 1 = 0 \quad (39)$$

To simplify, let:

$$b = \left(\frac{C_1}{C_2}\right)^{1/2} \cos Y_k \geq 1 \quad (40)$$

Then:

$$\left[\left(\frac{R_1}{R_2}\right)^{1/2}\right]^2 - 2b\left(\frac{R_1}{R_2}\right)^{1/2} + 1 = 0 \quad (41)$$

Solving the quadratic for  $(R_1/R_2)^{1/2}$ :

$$\left(\frac{R_1}{R_2}\right)^{1/2} = b \pm (b^2 - 1)^{1/2} \quad (42)$$

or

$$\frac{R_1}{R_2} = [b + (b^2 - 1)^{1/2}]^2 \quad (43)$$

This gives way to the following design procedure.

Due to the constraint on  $b$ , the following applies:

$$\frac{C_1}{C_2} \geq \frac{1}{\cos^2 Y_k} = 4Q_k^2 \quad (44)$$

Therefore, choose  $C_1$  and  $C_2$  such that:

$$C_1 \geq \frac{C}{\cos Y_k} = 2Q_k C \quad (45)$$

$$C_2 \leq C \cos Y_k = \frac{C}{2Q_k} \quad (46)$$

where  $C$  determines the range of capacitance desired. From that,  $b$  can be calculated in order to find:

$$R_1 = \frac{b + (b^2 - 1)^{1/2}}{2\pi f_c (C_1 C_2)^{1/2}} \quad (47)$$

$$R_2 = \frac{b - (b^2 - 1)^{1/2}}{2\pi f_c (C_1 C_2)^{1/2}} \quad (48)$$

$$\text{where: } f_c = \left[ \frac{f_p}{(10^{a_p/10} - 1)^{1/2n}} * \frac{f_s}{(10^{a_s/10} - 1)^{1/2n}} \right]^{1/2} \quad (49)$$

In order to complete the design, the number of poles,  $n$ , needed to fit the specifications must be found.

$$n \geq \frac{\log[(10^{a_s/10} - 1)/(10^{a_p/10} - 1)]}{2\log(f_s/f_p)} \quad (50)$$

The Butterworth angles,  $Y_k$ , are defined by two simple

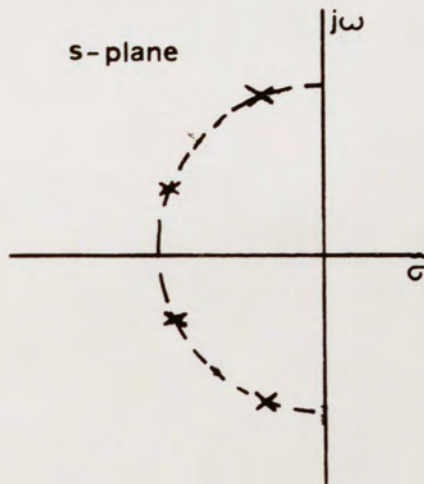


Figure 26. Pole Locations on Unit Circle.

rules:

1. For  $n$  odd, one pole is at 0 degrees. For  $n$  even, two poles are at  $+ \text{ or } - 90 \text{ deg}/n$ .
2. Poles are separated by  $180 \text{ deg}/n$ .

Therefore, for four poles, the corresponding Butterworth angles are  $+ \text{ or } - 22.5^\circ$  and  $+ \text{ or } - 67.5^\circ$ , and the pole locations on the unity circle are shown in Figure 26.

The following is a quick summary of the design for the

lowpass filter.

Specifications:  $a_s = 40$  dB  $f_s = 60$  Hz  
 $a_p = 0.5$  dB  $f_p = 10$  Hz

Find  $f_c$  using eqn. 49:  $f_c = 15.71002$  Hz

Find  $n$  using eqn. 50:  $n \geq 3.157$  choose  $n = 4$

Butterworth angles:  $Y_0 = 22.5^\circ$   $\cos Y_0 = 0.92388$   
 $Y_1 = 67.5^\circ$   $\cos Y_1 = 0.38368$

Find component values using eqns. 45, 46, 40, 47 and 48 for  $C_1$ ,  $C_2$ ,  $b$ ,  $R_1$  and  $R_2$ , respectively; Let  $C = 0.1$  uf:

Stage 0:  $C_1 \geq 1.082E-7$  choose  $C_1 = 0.22$  uf  
 $C_2 \leq 0.9238E-7$  choose  $C_2 = 68$  nf  
 $b = 1.661775$   
 $R_1 = 247.57E3$  choose  $R_1 = 240$  kohm  
 $R_2 = 27.711E3$  choose  $R_2 = 27$  kohm

Repeat for next stage.

Stage 1:  $C_3 \geq 2.613E-7$  choose  $C_3 = 0.47$  uf  
 $C_4 \leq 0.3827E-7$  choose  $C_4 = 22$  nf  
 $b = 1.7687938$   
 $R_3 = 321.57E3$  choose  $R_3 = 330$  kohm  
 $R_4 = 30.866E3$  choose  $R_4 = 30$  kohm

The highpass design is achieved using a lowpass design and RC-CR transformation (Van Valkenburg 1982). The component values are switched as follows:

$$R_j = 1/C_j \quad \text{and} \quad C_j = 1/R_j$$

Consequently, a second order highpass stage (Figure 27) has the same transfer function as a lowpass stage except for an  $s^2$  term in the numerator. This implies pole reciprocation has taken place, or, in other words, an equal number of zeros have been added to the origin in the complex plane as

illustrated in Figure 28.

Design of a Butterworth highpass is less complicated since an equal capacitor design can be used. The resistor values are dependent on the Butterworth angles:

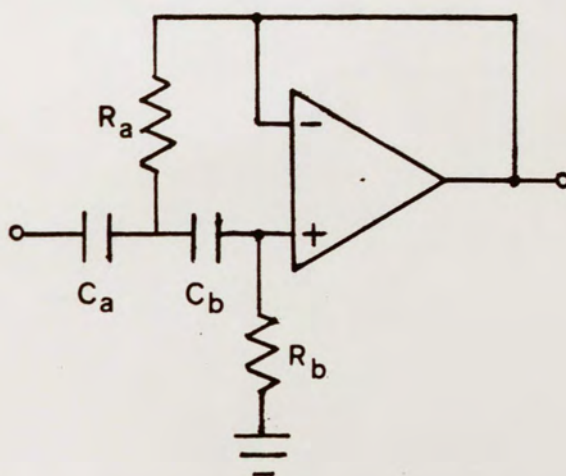


Figure 27. Sallen and Key Highpass Stage (Second Order).

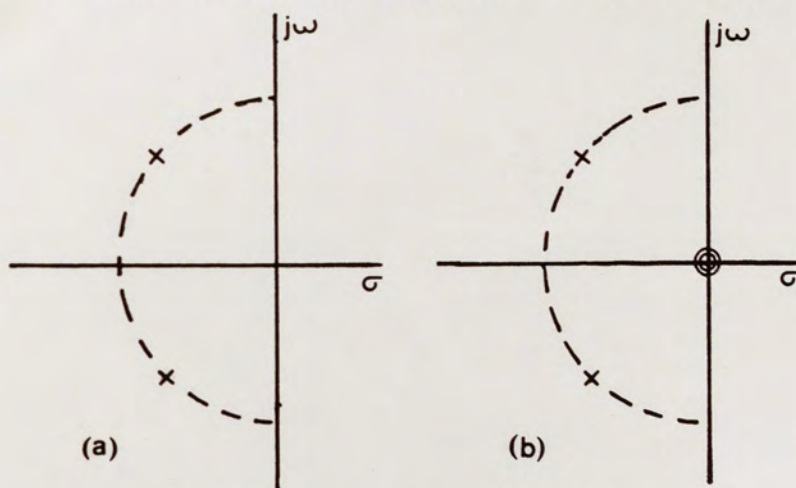


Figure 28. Pole Reciprocation (a)Lowpass to (b)Highpass.

$$R = 1/(w_o C) \quad (51)$$

$$R_1 \geq R \cos Y_k \quad (52)$$

$$R_2 \leq \frac{R}{\cos Y_k} \quad (53)$$

The number of stages needed,  $n$ , is found through the same equation as the lowpass.

Specifications:  $a_s = 40$  dB  $f_s = 0.1$  Hz  
 $a_p = 0.5$  dB  $f_p = 1$  Hz

Find  $n$  using eqn. 50:  $n \geq 2.4567$  choose  $n = 4$

Butterworth angles: same as lowpass

Let:  $C_5 = C_6 = C_7 = C_8 = C = 1$  uf

Find  $R$  using eqn. 51:  $R = 784.73E3$

Find resistor values using eqns. 52 and 53:

Stage 0:  $R_5 \geq 724.995E3$  choose  $R_5 = 750$  kohm  
 $R_6 \leq 849.383E3$  choose  $R_6 = 820$  kohm

Stage 1:  $R_7 \geq 300.303E3$  choose  $R_7 = 300$  kohm  
 $R_8 \leq 2.0505E6$  choose  $R_8 = 2$  Mohm

The final design is shown in figure 10 on page 20.

APPENDIX D  
SPECTRUM ANALYZER DATA

APPENDIX D

MEASUREMENTS OF FREQUENCY RESPONSE ON AN  
HP 3582A SPECTRUM ANALYZER

Channel 1

Frequency Range: 0 to 1 Hz

No. of Data Points: 64

<u>Freq (Hz)</u>	<u>Magn (dB)</u>	<u>Freq (Hz)</u>	<u>Magn (dB)</u>
0.128	- 15.0	0.392	- 0.8
0.136	- 13.0	0.400	- 0.8
0.144	- 11.4	0.408	- 0.8
0.152	- 10.0	0.416	- 0.8
0.160	- 8.8	0.424	- 0.8
0.168	- 7.7	0.432	- 0.8
0.176	- 6.6	0.440	- 0.7
0.184	- 5.5	0.448	- 0.7
0.192	- 4.7	0.456	- 0.7
0.200	- 4.0	0.464	- 0.7
0.208	- 3.6	0.472	- 0.7
0.216	- 3.2	0.480	- 0.6
0.224	- 2.8	0.488	- 0.6
0.232	- 2.5	0.496	- 0.6
0.240	- 2.2	0.504	- 0.6
0.248	- 2.0	0.512	- 0.6
0.256	- 1.8	0.520	- 0.6
0.264	- 1.6	0.528	- 0.6
0.272	- 1.6	0.536	- 0.6
0.280	- 1.6	0.544	- 0.6
0.288	- 1.5	0.552	- 0.6
0.296	- 1.3	0.560	- 0.6
0.304	- 1.2	0.568	- 0.5
0.312	- 1.2	0.576	- 0.5
0.320	- 1.2	0.584	- 0.5
0.328	- 1.1	0.592	- 0.5
0.336	- 1.1	0.600	- 0.5
0.344	- 1.0	0.680	- 0.4
0.352	- 1.0	0.704	- 0.4
0.360	- 1.0	0.792	- 0.4
0.368	- 0.9	0.832	- 0.3
0.376	- 0.9	0.984	- 0.3
0.384	- 0.9	1.016	- 0.3



Channel 1

Frequency: 0 to 25 Hz

No. of Data Points: 64

<u>Freq (dB)</u>	<u>Magn (Hz)</u>	<u>Freq (dB)</u>	<u>Magn (Hz)</u>
0.0	- 5.6	14.0	- 3.2
0.2	- 3.7	14.2	- 3.4
0.4	- 2.0	14.4	- 3.7
0.6	- 0.9	14.8	- 4.3
0.8	- 0.6	15.2	- 4.7
1.0	- 0.6	15.6	- 5.2
1.2	- 0.7	16.0	- 5.7
1.4	- 0.6	16.4	- 6.3
1.6	- 0.5	16.8	- 6.9
1.8	- 0.3	17.2	- 7.6
2.0	- 0.2	17.6	- 8.2
2.4	- 0.1	18.0	- 8.8
3.0	- 0.2	18.4	- 9.4
3.4	- 0.1	18.8	- 10.1
4.6	- 0.2	19.2	- 10.7
5.0	- 0.1	19.6	- 11.3
5.6	- 0.2	20.0	- 11.9
5.8	- 0.1	20.4	- 12.5
6.0	- 0.2	20.8	- 13.1
6.8	- 0.3	21.2	- 13.7
7.0	- 0.2	21.6	- 14.3
8.0	- 0.3	22.0	- 15.0
9.0	- 0.4	22.4	- 15.5
9.2	- 0.5	22.6	- 15.7
9.6	- 0.6		
10.4	- 0.7		
10.6	- 0.8		
11.0	- 0.9		
11.2	- 1.0		
11.4	- 1.1		
11.6	- 1.2		
11.8	- 1.3		
12.0	- 1.4		
12.2	- 1.6		
12.4	- 1.7		
12.6	- 1.8		
12.8	- 2.0		
13.0	- 2.2		
13.2	- 2.4		
13.4	- 2.5		
13.6	- 2.6		
13.8	- 2.9		

Channel 2

Frequency Range: 0 to 1 Hz

No. of Data Points: 64

<u>Freq (Hz)</u>	<u>Magn (dB)</u>	<u>Freq (Hz)</u>	<u>Magn (dB)</u>
0.144	- 14.3	0.392	- 1.0
0.152	- 12.4	0.400	- 1.0
0.160	- 10.8	0.408	- 0.9
0.168	- 9.5	0.416	- 0.9
0.176	- 8.4	0.424	- 0.9
0.184	- 7.5	0.432	- 0.8
0.192	- 6.7	0.448	- 0.8
0.200	- 5.9	0.464	- 0.8
0.208	- 5.0	0.472	- 0.7
0.216	- 4.2	0.496	- 0.7
0.224	- 3.5	0.514	- 0.7
0.232	- 3.1	0.536	- 0.7
0.240	- 2.8	0.544	- 0.6
0.248	- 2.6	0.568	- 0.6
0.256	- 2.4	0.616	- 0.6
0.264	- 2.3	0.624	- 0.5
0.272	- 2.1	0.656	- 0.5
0.280	- 1.9	0.712	- 0.5
0.288	- 1.7	0.720	- 0.4
0.296	- 1.5	0.744	- 0.4
0.320	- 1.5	0.792	- 0.4
0.328	- 1.4	0.824	- 0.4
0.336	- 1.3	0.872	- 0.4
0.344	- 1.1	0.880	- 0.3
0.360	- 1.1	0.928	- 0.3
0.376	- 1.1	0.976	- 0.3
0.384	- 1.1	1.016	- 0.3

Channel 2

Frequency Range: 0 to 25 Hz

No. of Data Points: 64

<u>Freq (Hz)</u>	<u>Magn (dB)</u>	<u>Freq (Hz)</u>	<u>Magn (dB)</u>
0.0	- 10.1	13.2	- 1.3
0.2	- 5.0	13.8	- 1.8
0.4	- 2.6	14.4	- 2.4
0.6	- 1.6	15.0	- 3.0
0.8	- 0.7	15.6	- 3.8
1.0	- 0.3	16.2	- 4.5
1.2	0.0	16.6	- 5.3
1.4	0.0	17.0	- 5.8
1.6	- 0.1	17.4	- 6.4
1.8	- 0.2	17.8	- 6.9
2.0	- 0.2	18.2	- 7.6
2.2	- 0.1	18.6	- 8.2
6.4	- 0.1	19.0	- 8.8
6.6	0.0	19.4	- 9.4
8.2	0.0	19.8	- 10.1
8.4	- 0.1	20.2	- 10.7
8.6	0.0	20.6	- 11.3
8.8	0.0	21.0	- 11.8
9.0	- 0.1	21.4	- 12.5
10.0	- 0.1	21.8	- 13.1
10.2	- 0.2	22.2	- 13.7
10.6	- 0.2	22.6	- 14.2
10.8	- 0.3	23.0	- 14.9
11.0	- 0.3	23.4	- 15.4
11.2	- 0.4	23.8	- 16.0
11.8	- 0.6		
12.2	- 0.7		
12.6	- 1.0		

## LIST OF REFERENCES

- Apple Computer Inc. 1981. Apple II Reference Manual. California: Apple Computer Inc.
- Godfrey, P. J. 1985. Interfacing a Quadriplegic to a Computer Using the Electro-Oculometer. Master's Thesis. University of Central Florida, Orlando, Florida.
- Gray, P. R. and Meyer, R. G. 1984. Analysis and Design of Analog Integrated Circuits. New York: John Wiley and Sons.
- Panayiotou, C. A. 1984. Design of an Evaluation System for the Electro-Oculometer. Master's Thesis. University of Central Florida, Orlando, Florida.
- Solomon, R. A. 1985. Optimum Input Impedance for an Electro-Oculometer. Master's Thesis. University of Central Florida, Orlando, Florida.
- Spectrum Software. 1983. Micro-Cap: Microcomputer Circuit Analysis Program. California: Spectrum Software.
- Van Valkenburg, M. E. 1982. Analog Filter Design. New York: Holt, Rinehart and Winston.
- Yarbus, A. 1967. Eye Movements and Vision. New York: Plenum Press.